Search for Antiproton Decay at the Fermilab Antiproton Accumulator

S. Geer, J. Marriner, R. Ray, and J. Streets
Fermi National Accelerator Laboratory, Batavia, Illinois 60510

M. Lindgren, Th. Muller, and J. Quackenbush
University of California, Los Angeles, California 90024-1547

T. Armstrong
Pennsylvania State University, University Park, Pennsylvania 16802

(T861 Collaboration)

(Received 27 October 1993)

A search for antiproton decay has been made at the Fermilab antiproton accumulator. Limits are placed on five antiproton decay modes. At the 95% C.L. we find that $\tau_{\bar{p}}/B(\bar{p}\rightarrow e^-\gamma) > 1848$ yr, $\tau_{\bar{p}}/B(\bar{p}\rightarrow e^-\pi^0) > 554$ yr, $\tau_{\bar{p}}/B(\bar{p}\rightarrow e^-\eta) > 171$ yr, $\tau_{\bar{p}}/B(\bar{p}\rightarrow e^- K_S^0) > 29$ yr, and $\tau_{\bar{p}}/B(\bar{p}\rightarrow e^- K_L^0) > 9$ yr.

PACS numbers: 13.30.Ce, 11.30.Er, 11.30.Fs, 14.20.Dh

There has been a considerable experimental effort devoted to the search for proton decay. As a result we know that the proton lifetime $\tau_p \gtrsim 10^{32}$ yr [1]. The *CPT* theorem requires that the proton and $\bar{p}$ lifetimes are equal. A search for $\bar{p}$ decay with a short lifetime ($\tau_{\bar{p}} < \tau_p$) tests both the *CPT* theorem and the intrinsic stability of antimatter.

There have been a number of searches for the decay of antiprotons stored in ion traps [2] and storage rings [3]. The most stringent published limit, $\tau_{\bar{p}} > 3.4$ months [2], was obtained by setting a limit on the containment lifetime of ≈ 1000 antiprotons stored in an ion trap. In addition to these direct searches for $\bar{p}$ decay, cosmic ray experiments can search indirectly. The observation of cosmic ray antiprotons with rates consistent with secondary production in the interstellar medium would imply that $\gamma\tau_{\bar{p}} > T$, where γ is the Lorentz factor, and T is the $\bar{p}$ confinement time within the galaxy ($\sim 10^7$ yr). Although earlier balloon experiments reported the observation of low energy antiprotons, a more recent experiment with greater sensitivity failed to observe a signal. One balloon experiment searching at higher $\bar{p}$ energies ($\gamma \geq 4$) has reported [4] the observation of cosmic ray antiprotons; however, the experiment lacked particle identification and its ability to identify antiprotons has been questioned. Hence, there is no confirmed limit on $\tau_{\bar{p}}$ from cosmic ray experiments.

In this paper we describe a new search for $\bar{p}$ decay. The experiment was performed at the Fermilab antiproton accumulator, operating with a beam momentum of 8.9 GeV/c, beam currents in the range 20–30 mA (1 mA in the accumulator corresponds to 10^{10} stored antiprotons), and typical beam lifetimes of 300 h. The detector was located downstream of a 15.9 m straight section in the 474 m circumference accumulator ring. The experimental setup [Fig. 1(a)] consisted of the following.

(i) A 5 m long stainless steel vacuum pipe with an inner diameter of 3 in. and a wall thickness of 0.7 mm. The measured pressures at the upstream and downstream pipe ends were respectively $(3^{+3.0}_{-1.5})\times 10^{-10}$ Torr and $(8^{+8}_{-4})\times 10^{-11}$ Torr. A mass spectrometer analysis of the residual gas showed the presence of H_2 (2×10^{-10} Torr), CH_4 (7×10^{-12} Torr), H_2O (4×10^{-11} Torr), CO (2×10^{-11} Torr), and CO_2 (1×10^{-11} Torr).

(ii) The forward electromagnetic calorimeter of the E760 experiment [5]. The calorimeter consists of 144 rectangular modules arranged in a 13×13 array with 6 modules at each of the 4 corners missing, and the central module absent to enable passage of the beam pipe. Each

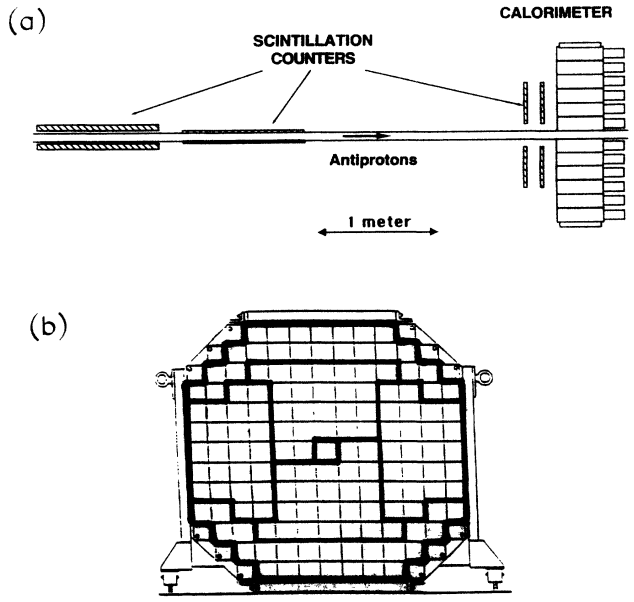

FIG. 1. Experimental setup: (a) side view and (b) calorimeter face showing the cell structure and cell groupings into six trigger sectors.

0031-9007/94/72(11)/1596(4)$06.00

module consists of 148 alternate layers of lead and acrylic scintillator plates with transverse dimensions of 10×10 cm^2. The lead plates are 1 mm thick. The first 32 scintillator plates are 6.4 mm thick and the remaining 42 plates are alternately 6.4 and 3.2 mm thick. The active length of the module is 48.4 cm (17.7 radiation lengths). Light is transported to a photomultiplier tube mounted behind each module via a wavelength shifter plate mounted on one side of the module. The response of the calorimeter to electrons and photons has been measured [5] by the E760 collaboration. The energy resolution is given by $\sigma/E=0.2/\sqrt{E\,[\mathrm{GeV}]}$. The calorimeter's linearity has been checked using 1 and 3 GeV electron beams. In this energy range nonlinearities do not exceed a few percent. The calorimeter's response to neutrons and charged hadrons is less precise. The measured energies of these particles tend to be less than their real energies since most hadronic showers are not fully contained within the calorimeter. The response of the calorimeter to neutrons and charged hadrons has not been measured directly. However, the beam-gas Monte Carlo program described below gives a good description of the calorimeter total energy (E_{tot}) distribution measured for antiprotons interacting in a gas-jet target. This gives us confidence that the calorimeter's response is understood and that our Monte Carlo program correctly predicts the E_{tot} distribution for $\bar{p}$-gas interactions at 8.9 GeV/c. In our $\bar{p}$-decay experiment the calorimeter energy scale was determined to $\pm2\%$ by comparing the measured E_{tot} distribution with the Monte Carlo prediction. The $\pm2\%$ uncertainty reflects the statistical uncertainties on the E_{tot} distributions, and also takes account of the level of agreement between the predicted and measured distributions for the gas-jet target data.

(iii) Additional scintillation counters. In particular four 1 m$\times$10 cm counters surrounding and adjacent to the beampipe were positioned with their long axes parallel to the beam direction and their downstream ends 2 m upstream of the calorimeter. Correlations between hits in these counters (up, down, left, right) and cluster positions in the calorimeter confirmed that particles depositing energy in the calorimeter come predominantly from interactions along the $\bar{p}$ orbit.

The calorimeter cells were grouped into six trigger sectors [Fig. 1(b)]. The trigger required that the energy deposited in the sector with the largest energy deposition E_{trig} exceed a threshold value, which was adjusted within the range 1.5–2.5 GeV. Data were taken for 5 h over a one week period during intervals when additional antiprotons were not being added to the accumulator and beam conditions were stable. The experiment recorded 6.8×10^6 events. During data taking the beam current was monitored and the number of antiprotons $N_{\bar{p}}(t)$ determined to better than 1%. The number of stored antiprotons integrated over the live-time of the experiment was $\int N_{\bar{p}}(t)dt=(1.280\pm0.013)\times10^8$ yr. Offline, after applying final calorimeter calibrations, the quantity E_{trig} was recalculated and events with $E_{\mathrm{trig}}>4$ GeV selected for further analysis. 2×10^6 events passed this requirement.

To compare event rates and properties with expectations for beam-gas interactions we have developed a Monte Carlo program which generates multipion final states for annihilation processes with up to eleven final state particles and nonannihilation processes with up to nine final state particles. Coulomb scattering has been implemented taking into account the measured residual gas composition in the beampipe. The generator uses published measurements of exclusive, semi-inclusive, and topological cross sections for $\bar{p}p$ [6] and $\bar{p}n$ [7] interactions at ≈8.9 GeV/c, and the measured kinematics for elastic scattering and for three-body nonannihilation final states. All other processes have been generated with a longitudinal phase space generator, with the particle mean transverse momenta adjusted to reproduce, as a function of final state multiplicity, the measured transverse momenta in annihilation and nonannihilation events. Beam-gas interactions were generated along the $\bar{p}$ orbit from 19 m upstream to 1 m downstream of the calorimeter, and the GEANT [8] Monte Carlo program used to track generated particles through the detector and simulate, as a function of particle type, the energy deposited in the calorimeter and the resulting calorimeter response.

The beam-gas Monte Carlo program predicts a trigger rate ($E_{\mathrm{trig}}>4$ GeV) of 55^{+55}_{-28} Hz when there are 2.6×10^{11} antiprotons in the accumulator, where the uncertainty on the prediction reflects the uncertainty on the vacuum inside the beampipe. The predicted rate is in good agreement with the measured rate of 72 Hz, which suggests that the recorded events originate predominantly from beam-gas interactions. The Monte Carlo program gives a reasonable description of the E_{tot} distribution [Fig. 2(a)], and also describes the distribution of calorimeter cell energies over an interval in which the rate falls by more than 3 orders of magnitude [Fig. 2(b)]. To further compare the event characteristics with the Monte Carlo predictions we define the following.

(a) The number of calorimeter clusters, N_C. The cluster finder forms a cluster by associating all cells within a 3×3 grid around the highest energy seed cell. Seed cells are defined as cells which have an energy $E_i>50$ MeV, and have not been previously associated with a cluster. Clustering is repeated until no seed cells remain.

(b) The energy imbalance, $S\equiv(E_X^2+E_Y^2)^{1/2}/E_{\mathrm{tot}}$, where $E_X=\sum_i E_i x_i/(x_i^2+y_i^2)^{1/2}$. $E_Y=\sum_i E_i y_i/(x_i^2+y_i^2)^{1/2}$, and the ith cell is located at position (x_i,y_i) with respect to the beam axis. The Monte Carlo predictions for N_C and S give a reasonable description of the data (Fig. 3). We conclude that the recorded events arise predominantly from beam-gas interactions.

In contrast to the majority of the observed events, we would expect that two-body $\bar{p}$ decays in which both decay products deposit all of their energy in the calorimeter

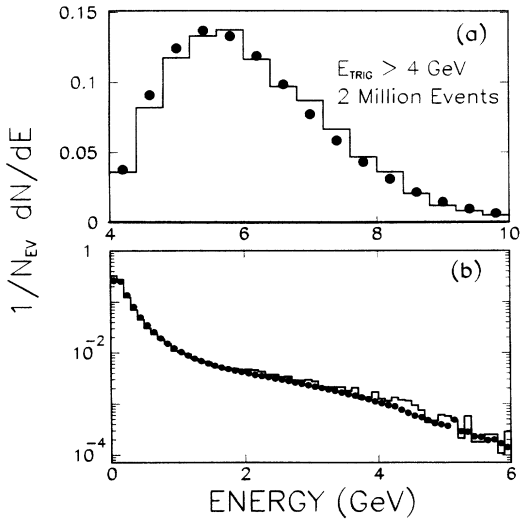

FIG. 2. Energy distributions for events with $E_{trig} > 4$ GeV: (a) calorimeter total energy distribution and (b) distribution of calorimeter cell energies. Data (points) are compared with predictions from the beam-gas Monte Carlo simulation (histogram).

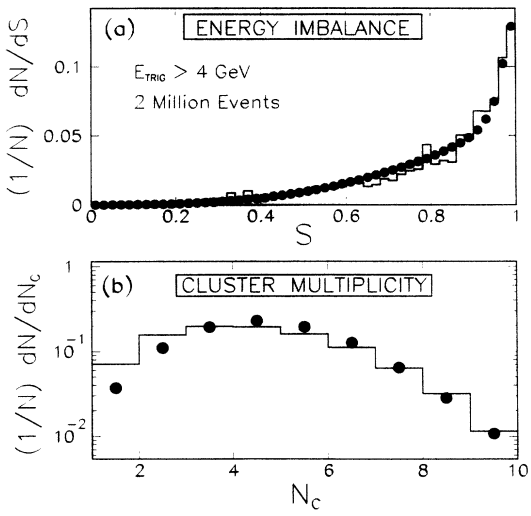

FIG. 3. Distributions of (b) cluster multiplicity and (a) energy imbalance as defined in the text. The data (points) are compared with the beam-gas Monte Carlo predictions (histogram).

would result in well balanced events with two calorimeter clusters and $8 < E_{tot} < 10$ GeV. As an example, in Fig. 4(a) the measured E_{tot} distribution for events passing the loose energy balance requirement $S < 0.5$ is compared with the Monte Carlo prediction for $\bar{p} \to e^- \pi^0$ decay with $\tau_{\bar{p}}/B(\bar{p} \to e^- \pi^0) = 3.4$ months. The data clearly exclude $\tau_{\bar{p}}/B(\bar{p} \to e^- \pi^0) = 3.4$ months. The sensitivity of the search for $\bar{p} \to e^- \pi^0$ decay can be improved by requiring well balanced events ($S < 0.1$) with $N_C = 2$. Three events survive these cuts, of which only one event has $8 < E_{tot} < 10$ GeV [Fig. 4(b)].

To extract a limit on $\bar{p} \to e^- \pi^0$ decay we consider the event with $N_C = 2$, $S < 0.1$, and $8 < E_{tot} < 10$ GeV to be a signal. Let the number of events passing the cuts be N, and the Poisson upper limit on N be N_{max}. We have $N = 1$ and $N_{max} = 4.74$ (95% C.L.). The limit on $\tau_{\bar{p}}/B$ is given by

$$\tau_{\bar{p}}/B > \frac{\varepsilon}{\gamma} \frac{1}{N_{max}} \int N_{\bar{p}}(t) dt , \qquad (1)$$

where the Lorentz factor $\gamma = 9.538 \pm 0.010$ and ε is the fraction of decays taking place uniformly around the accumulator ring that would pass the trigger and event selection requirements. The GEANT Monte Carlo program has been used to simulate the detector response and calculate ε. We find that $\varepsilon = (2.19 \pm 0.20 \pm 0.07) \times 10^{-4}$, where the first error is statistical and the second error reflects the uncertainty on ε due to the uncertainty on the calorimeter energy scale. As an additional check the event selection has been repeated with the calorimeter energy scale changed by ± 1 standard deviations ($\pm 1\sigma$). When this is done, there is no increase in the number of events passing the selection cuts. Note that the uncertainties on ε, γ, and $N_{\bar{p}}(t)$ are negligible compared with the statistical uncertainty associated with the observation of one event. We could therefore neglect the uncertainties on ε, γ, and $N_{\bar{p}}(t)$ and use expression (1) to extract a 95% C.L. on $\tau_{\bar{p}}/B$. However, we choose a more conservative approach. We reduce ε and $N_{\bar{p}}(t)$ by 1σ and increase γ by 1σ. At the 95% C.L. expression (1) then yields the limit $\tau_{\bar{p}}/B(\bar{p} \to e^- \pi^0) > 554$ yr.

In addition to $\bar{p} \to e^- \pi^0$ there are several other two-

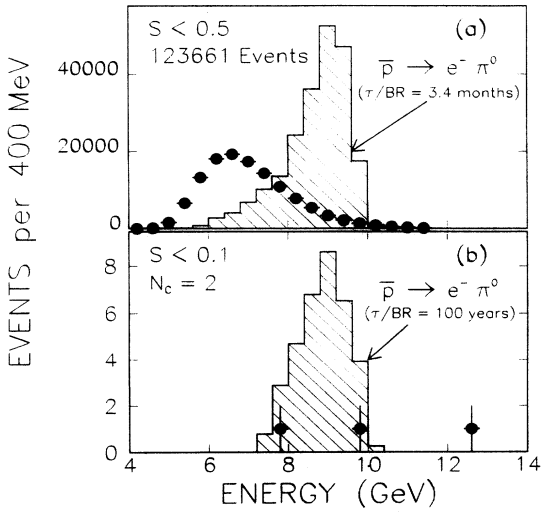

FIG. 4. Calorimeter energy distributions (points) compared with Monte Carlo predictions for $\bar{p} \to e^- \pi^0$ decay for (a) events passing a loose energy balance requirement and (b) events with two clusters and energy imbalance $S < 0.1$.

TABLE I. Efficiencies and limits on $\tau_{\bar{p}}/B$ for five decay modes of the antiproton. The uncertainties on the calculated ε are statistical and systematic, respectively.

Mode	ε	Limit (95% C.L.) (yr)
$\bar{p}\to e^-+\gamma$	$(6.95\pm0.33\pm0.09)\times10^{-4}$	1848
$\bar{p}\to e^-+\pi^0$	$(2.19\pm0.20\pm0.07)\times10^{-4}$	554
$\bar{p}\to e^-+\eta$	$(7.00\pm0.77\pm0.40)\times10^{-5}$	171
$\bar{p}\to e^-+K_S^0$	$(1.27\pm0.23\pm0.07)\times10^{-5}$	29
$\bar{p}\to e^-+K_L^0$	$(4.6\pm1.4\pm0.2)\times10^{-6}$	9

body decay modes which would result in events with $S<0.1$, $N_C=2$, and $8<E_{\rm tot}<10$ GeV; namely, $\bar{p}\to e^-X$, where $X=\gamma$, η, K_S^0, or K_L^0. For each mode the GEANT Monte Carlo program has been used to simulate the detector response and calculate ε. The calculated ε and the resulting lower limits on $\tau_{\bar{p}}/B$ are listed in Table I. The most stringent limit is for the decay $\bar{p}\to e^-\gamma$. At the 95% C.L. we find that $\tau_{\bar{p}}/B(\bar{p}\to e^-\gamma)>1848$ yr.

We thank the Fermilab Accelerator and Physics Division staff for their support and encouragement. We also wish to acknowledge the cooperation of the E760 collaboration which enabled us to use existing readout and data acquisition systems. This work was supported by the Department of Energy and the National Science Foundation.

[1] Particle Data Group, K. Hikasa *et al.*, Phys. Rev. D **45**, S1 (1992).
[2] G. Gabrielse *et al.*, Phys. Rev. Lett. **65**, 1317 (1990).
[3] M. Bregman *et al.*, Phys. Lett. **78B**, 174 (1978); M. Bell *et al.*, Phys. Lett. **86B**, 215 (1979).
[4] R. L. Golden *et al.*, Phys. Rev. Lett. **43**, 1196 (1979).
[5] M. A. Hasan *et al.*, Nucl. Instrum. Methods Phys. Res., Sect. A **295**, 73 (1990).
[6] P. S. Gregory *et al.*, Nucl. Phys. **B119**, 60 (1977); A. J. Simmons *et al.*, Nucl. Phys. **B172**, 285 (1980); D. R. Ward *et al.*, Nucl. Phys. **B172**, 302 (1980).
[7] H. Braun *et al.*, in Proceedings of the 5th European Symposium on Nucleon Antinucleon Interactions, Bressanone, 1980, edited by M. Cresti (Istituto Nazionale di Fisica Nucleare, Padua, Italy, 1980).
[8] R. Brun *et al.*, CERN Data Handling Division, DD/EE/84-1, CERN-CN, CH-1211 Geneva 23, Switzerland.